IMU Based Serial Manipulator Joint Angle Monitoring: Comparison of Complementary and Double Stage Kalman Filter Data Fusion

Souha Baklouti, Taysir Rezgui, Asma Chaouch, Abdelbadiaa Chaker, Safa Mefteh, Anis Sahbani, Samir Bennour

IMU Based Serial Manipulator Joint Angle Monitoring: Comparison of Complementary and Double Stage Kalman Filter Data Fusion

Souha Baklouti[1,2*], Taysir Rezgui[3], Asma Chaouch[4], Abdelbadiaa Chaker[1], Safa Mefteh[2], Anis Sahbani[2,5], and Sami Bennour[1]

[1] Mechanical Laboratory of Sousse (LMS), National School of Engineers of Sousse, University of Sousse, Tunisia.

[2] ENOVA Robotics S.A., Novation City, Tunisia.

[3] Applied Mechanics and Systems Research Laboratory (LASMAP), Polytechnic School of Tunisia, University of Carthage, Tunisia.

[4] Laboratory of Electronic and Micro-electronics (EμE), Faculty of science of Monastir, University of Monastir, Tunisia.

[5] Sorbonne University, CNRS, Institute for Intelligent Systems and Robotics (ISIR), Paris, France.

*baklouti.souha@eniso.u-sousse.tn

Abstract. Inertial Measurement Units (IMU) are in highlight for joint and motion monitoring applications. Several IMU sensor fusion algorithms have been proposed in literature. Kalman Filter and its variants are the most used for more precision. However, they are computationally expensive. However, for faster computations, researchers and industry use complementary filter. More recently, a new variant of Kalman Filter was introduced as a Double Stage Kalman Filter in order to reduce the Kalman Filters computation cost. Our research investigates the performance of the Complementary and Double Stage Kalman filters in monitoring of joints in serial manipulators using Microelectromechanical-system MEMS based IMU. This study carried dynamic experiments using a serial robot to estimate the orientation of IMU, thus the joint angle of the associated segment. The study showed that both filters yield accurate estimations. The study showed also that Double Stage Kalman Filter has lower RMSE and achieves more precise estimates than Complementary filter mainly when the movement is around IMU x- and y- axis. Our findings indicate that the Double Stage Kalman Filter can achieve higher precision than the complementary filter using lower computation time than the former variants of the Kalman Filters in serial manipulator joint monitoring applications.

Keywords: Complementary Filter, Double Stage Kalman Filter, Data Fusion, Joint monitoring, Serial Manipulator.

1 Introduction

Information about a serial manipulator joint angle is crucial in applications including serial robots joint monitoring, human motion assessment, exoskeletons, etc. In this context, several techniques have been proposed by literature (Rosado et al. 2014; Choi et al. 2017; Littrell et al. 2018). Among all these techniques, the sensor fusion of Inertial Measurement Unit (IMU) is of importance since it provides information about joint motion from multi-sensor observations: gyroscope, accelerometer and, sometimes, magnetometer. While it is possible to obtain the relative orientation of the IMU from the gyroscope, the latter tends to drift over time. The orientation of the IMU can also be determined from the accelerometer and magnetometer with respect to the gravity and earth magnetic field. However, they can be very noisy. In this context, sensor fusion algorithms give solutions to compensate the gyroscope drift using accelerometer and magnetometer measurements. Several sensor fusion algorithms have been reported in literature. However, Kalman filter (KF) and complementary filter (CF) are the most used. KF is a highly efficient iterative filter, but it is very complex computationally. In fact, KF requires the knowledge of the mathematical model of the system, and it is very sensitive to its noise parameters (Kalman 1960). Although several variants of the KF have been made, they are still computationally complex (Wu 2019). In contrast, CF does not require any prior knowledge of the mathematical model of the system nor its environment. CF is based on inexpensive computations, and it is easy to implement (Colton 2007). Because of that, it is preferred for embedded applications. More recently, another variant of the KF, double stage Kalman filter (DSKF) was designed to overcome some of the KF issues (Sabatelli et al. 2012). Mainly, the reduction of the complexity of KF computations. This paper investigates the behavior of the CF and DSKF and their performance in estimating serial manipulator joint angles.

2 Methods

For this study, we used a 9-DoF MPU-9250 microelectromechanical System (MEMS) based IMU combining an accelerometer, a gyroscope, and a magnetometer. The gyroscope measures the rate of rotation around IMU x-, y- and z- axis. The accelerometer measures the acceleration by calculating the forces acting on the center of gravity along the IMU x-, y- and z- axis. The magnetometer measures the strength and direction of the magnetic field along x-, y- and z- axis. All three sensor types use MEMS hardware. This means that even if the device is in a static position the sensors will return values other than zero. Each sensor has its own unique bias sources and types (Novatel 2014). The static bias is caused by manufacturing and material characteristics. The value of this bias must be calculated

each time the sensor is powered up because it can change due to the initialization of the signal processor in the IMU. In addition, accelerometer, gyroscope, and magnetometer are capacitive sensors which measure data indirectly. This results in a scaling bias due to an incorrect scaling factor between the measured data and scaled output. The measurements of the Magnetometer are also sensitive to noise sources. The accuracy of these measurements is degraded by two disturbances: hard ion effects and soft ion effects. To correct the magnetometer measurements, difference between the measured magnetic field ellipsoid and a perfect sphere must be calculated. The gyroscope mathematical model is given by equation (1) where, $\tilde{\omega}$ is the data measured by the gyroscope; k_g is the scale factor of the gyroscope; ω is the true gyroscope rate; b_g is the static bias of the gyroscope; and n_g is a zero mean Gaussian noise corrupting the gyroscope measurements. The accelerometer mathematical model is given by equation (2) where $\tilde{a}$ is the data measured by the accelerometer; k_a is the scale factor of the accelerometer; a is the true acceleration; g is the gravitational acceleration; b_a is the static bias of the accelerometer; And η_a is a zero mean Gaussian noise corrupting the accelerometer measurements. The magnetometer mathematical model is given by equation (3) where $\tilde{m}$ is the data measured by the magnetometer; k_m is the scale factor of the magnetometer; m is the true magnetic field; A_m and b_m are the magnetometer calibration parameters.

$$\tilde{\omega} = k_g\,\omega + b_g + n_g \quad (1)$$

$$\tilde{a} = k_a a - g + b_a + \eta_a \quad (2)$$

$$\tilde{m} = (k_m m - b_m) * A_m \quad (3)$$

Needless to say, each sensor needs its biases calculated to allow for sensor calibration and measurements correction.

2.1. Complementary Filter

The CF was introduced by (Colton 2007) to compensate the drift of the gyroscope. Contrarily to the accelerometer and the magnetometer, the gyroscope is reliable on the short term. However, on the long term, the accelerometer becomes reliable but the gyroscope drifts. The CF takes advantage of the reliability of the gyroscope on the short term and accelerometer on the long term to estimate the orientation of the sensor. In fact, this filter applies a High-pass and a low pass filter on the data obtained from the gyroscope and the accelerometer, respectively. The high-pass filter lets through the short-duration reliable gyroscope data while filtering out the unreliable accelerometer data. The low-pass filter allows the passing of the long-duration reliable accelerometer signals but prevent the drifting gyroscope signals from passing through. This filter is implemented during the data fusion process within a loop as shown by fig. 1. Gyro data are integrated over time to yield an initial estimation of the IMU orientation. The equation (4) sums up the complementary filter. If the accelerometer data are within a proper magnitude interval and could be a real gravity force vector, the roll and pitch orientations are

updated with tilt angles estimated from the accelerometer. Otherwise, it will be considered as a disturbance. Similarly, we can update the yaw orientation with the tilt angle estimated from the magnetometer readings.

$$Orientation = \propto * Orientation + (1 - \propto) * [Roll_a \; Pitch_a \; Yaw_m] \quad (4)$$

The filter parameter α takes a value between 0 and 1. The lower this value is, the more the orientation estimation relies on the data obtained from the accelerometers. It is recommended to use a high α value, but it relies heavily on experience. In this study, we used α = 0.98.

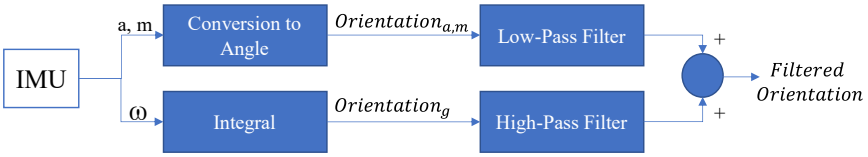

Fig. 1 Complementary filter data fusion flowchart.

Given that accelerometers measure the acceleration of the IMU, it is possible to determine the orientation with respect to gravity by calculating the ratio of the gravity measured along each axis. The equations (5) and (6) below describe the relationship between the accelerometer readings and the sensor orientation where, A_x, A_y and A_z are the calibrated accelerometer readings along the x-, y- and z-axis of the IMU respectively (Pedly 2013). Since the accelerometer determines the orientation with respect to the direction of the gravity, z-axis in this case, it is not possible to determine the yaw using it. That's why the magnetometer is commonly used to determine the yaw rotation. Since the earth magnetic field measured by the magnetometer is perpendicular to the direction of the gravity, it is possible to determine the rotation in the horizontal plane. Since the roll and pitch are different from zero when the sensor is tilted, the yaw rotation is therefore calculated using the equation (7), Where M_x, M_y and M_z are the calibrated magnetometer measurements along the x-, y- and z-axis of the IMU respectively.

$$Roll_a = Arctan\left(\frac{A_y}{\sqrt{A_x^2 + A_z^2}}\right) \quad (5)$$

$$Pitch_a = Arctan\left(-\frac{Ax}{\sqrt{A_y^2 + A_z^2}}\right) \quad (6)$$

$$Yaw_m = Arctan\left(-\frac{M_y Cos(roll) + M_z Sin(roll)}{M_x Cos(pitch) + M_y Sin(roll) + M_z \, Cos(roll) Sin(pitch)}\right) \quad (7)$$

2.2. Double stage Kalman Filter

DSKF was introduced by (Sabatelli *et al.*, 2012) to reduce the complexity of KF algorithms. As its name indicates, the data fusion is performed by dividing the KF into two stages: the first stage deals with the corrections using the accelerometer,

and the second stage deals with the corrections using the magnetometer. The filter is iterative, and it is implemented as explained by the Fig. 2. The data obtained from the gyroscope are used to obtain an initial estimation of the IMU orientation. The orientation of the system with respect to its inertial frame is described using quaternion algebra. The equation (8) represents the state equation of the IMU with respect to its inertial frame, where $A_k = (I + \frac{1}{2}\Omega_k \Delta t)$ and Ω_k is the rotational matrix formed by the angular velocities measured by the gyroscope at iteration k; Δt is the time between two iterations and $q(k-1)$ is the quaternion representing the rotation of the IMU at the previous iteration.

$$q(k) = A_k q(k-1) \tag{8}$$

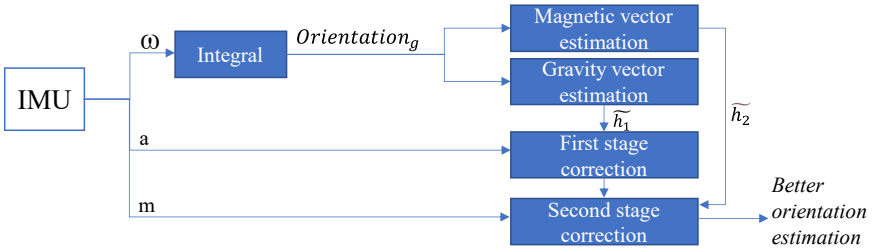

Fig. 2 Double stage Kalman filter data fusion flowchart.

The first stage estimates the roll and pitch orientations of the IMU by the means of the comparison of the accelerometer data with the estimated gravity vector. Knowing the equation (8), the estimated gravity vector at the iteration k can be determined by the equation (9).

$$\widetilde{h_1}(k) = |g| \begin{bmatrix} 2q_2(k)q_4(k) - 2q_1(k)q_3(k) \\ 2q_1(k)q_2(k) + 2q_3(k)q_4(k) \\ q_1^2(k) - q_2^2(k) - q_3^2(k) + q_4^2(k) \end{bmatrix} \tag{9}$$

The correction quaternion, q_{e1k}, is calculated by the means of the multiplication of the difference between the accelerometer data and the estimated gravity vector, $\widetilde{h_1}(k)$, by a first computed Kalman gain. To make sure that the yaw orientation is not affected by the correction using the accelerometers, the fourth element of the correction quaternion q_{e1k} is set to 0. A first correction of the estimated orientation quaternion is then obtained using equation (10). At the end of the first stage, the post error covariance matrix is updated.

$$q(k) = q(k) + \ q_{e1k} \tag{10}$$

The second stage estimates the yaw orientation of the IMU by the means of the comparison of the magnetometer data with the estimated magnetic vector. Similarly, knowing equation (8) the magnetic vector can be estimated using the equation (11).

$$\widetilde{h_2}(k) = \begin{bmatrix} 2q_2(k)q_3(k) + 2q_1(k)q_4(k) \\ q_1^2(k) - q_2^2(k) - q_3^2(k) - q_4^2(k) \\ 2q_3(k)q_4(k) - 2q_1(k)q_2(k) \end{bmatrix} \tag{11}$$

A second correction quaternion q_{2e} is calculated by the means of the multiplication of the difference between the magnetometer measurements and the estimated magnetic vector, $\widetilde{h_2}(k)$, by a second computed Kalman gain. Since the second stage deals only with the correction of the yaw orientation, the second and third elements of the correction quaternion q_{e2k} are set to 0. Finally, we obtain a second correction of the orientation quaternion estimate using equation (12). At the end of the second stage, the post error covariance matrix is updated.

$$q(k) = q(k) + \ q_{e2k} \tag{12}$$

3 Simulation

The CF and DSKF filters were implemented in a post data acquisition algorithm to test their behaviors and study the accuracy to which they can estimate the joint angles of a serial manipulator. For the simulation, we used an IMU MPU-9250, ARDUINO ATmega2560 microcontroller and a 5-axis SCORBOT ER-9 PRO robot. The aim of this simulation is investigating the performance of the two algorithms in determining the joint angles of the end effector of the robot. All calculations were performed with MATLAB software package. To monitor serial manipulators joints, IMUs are equipped to each segment. The IMU axis coinciding with the segment relative frame. After that rotation matrices can calculated using the Denavit-Hartenberg model (Denavit and Hartenberg 1955) and from the Euler angles obtained from the IMUs. The equality between the two matrices allows the calculation of joints angles from the data fusion results. For the experiment, the IMU was positioned on the end effector of the robot in a way that its axis coincides with the end effector joint axis to simplify calculations. In this study, the robot is maintained extended and only joint angles around the 1st, 2nd, and 5th axis of the robot are tested as demonstrated by the fig. 3. The change from encoder measurements to angles is done by multiplying these values by the resolution of the joint. The resolution of the joint is the smallest possible increment that the control system can identify and theoretically control. The resolution of the joint is determined by means of equation (13), where S_E is the resolution of the encoder and N_{AXIS} is the overall gear ratio of the axis (Interlink Inc 2011).

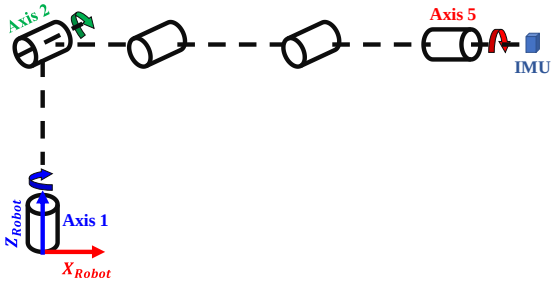

Fig. 3 SORBOT ER-9 PRO kinematics scheme and simulation test setup

$$S_{JOINT} = \frac{S_E}{N_{AXIS}} \tag{13}$$

For the simulation, 3 tests were performed. 5 repetitions of rotation around the IMU x-axis (Robot z-axis), the IMU y-axis (Robot y-axis) and the IMU z-axis (Robot x-axis) were performed and recorded during the 1st test (Fig. 4), 2nd test (Fig. 5), and 3rd test (Fig. 6), respectively. Three repetitions of each test were performed. We obtained averaged correlation coefficients r^2 between the encoder and the data obtained from the IMU of 0.993, 0.994 and 0.979 against 0.993, 0.993, and 0.978 for Θ_1, Θ_2, and Θ_3 estimated from the DSKF and the CF, respectively. Both filters show comparable and high r^2 coefficients indicating that both filters describe the variation in the joint angles accurately.

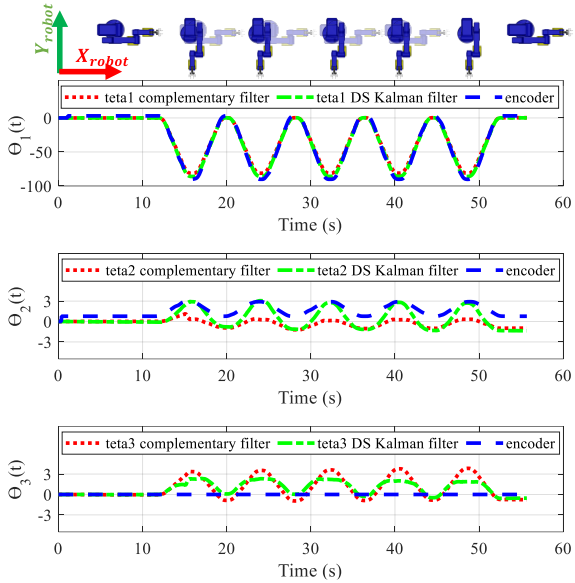

Fig. 4 Estimated joint angles during rotations around robot z-axis

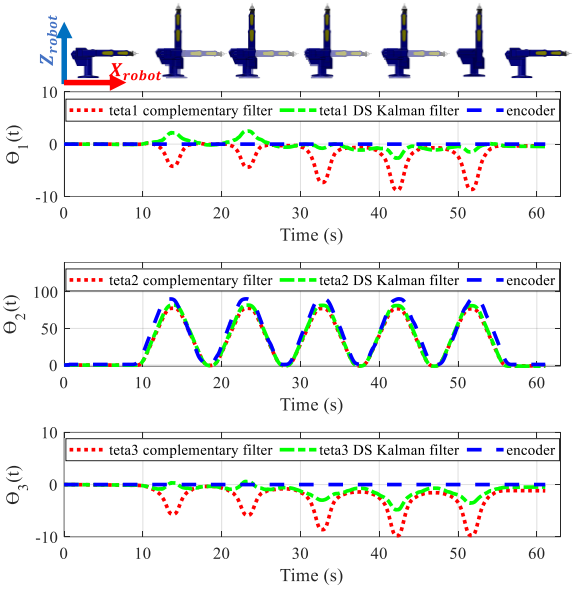

Fig. 5 Estimated joint angles during rotations around robot y-axis

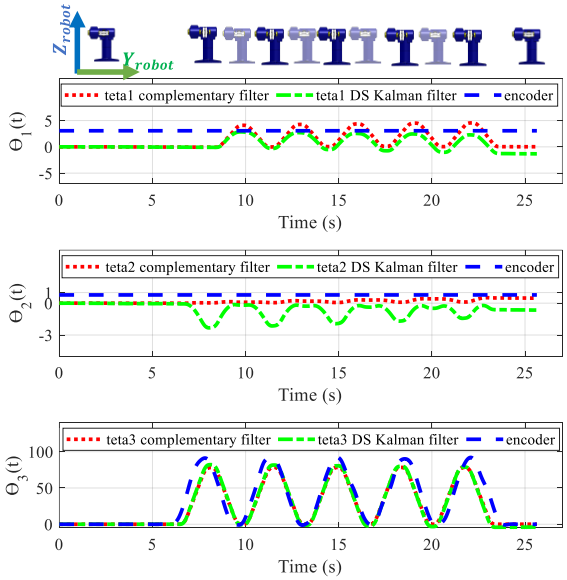

Fig. 6 Estimated joint angles during rotations around robot x-axis

The Fig. 7 shows the averaged root mean square error. This result indicates that DSKF estimates the joint angles around the 1st, 2^{nd,} and 5th axis of the robot with an RMSE of 1.8° ±0.9, 4.5° ±3, and 7.3° ±6 respectively. Compared to 3.5° ± 1.2, 4.9°

±4, and 7.5° ±6 estimated by CF around the 1st, 2nd, and 5th axis, respectively. Accordingly, the DSKF is more precise in estimating the joint angles especially for rotations around the 1st and 2nd axis of the robot, thus x- and y- axis of the IMU.

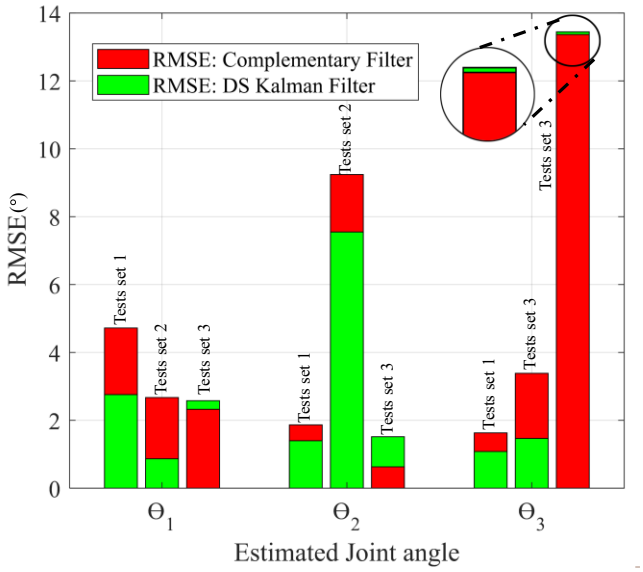

Fig. 7 Averaged RMSE of estimated joint angles during all tests.

4 Conclusion

In this study, we investigate the behavior of the complementary and double stage Kalman filters. These filters are computationally inexpensive and are commonly implemented in embedded applications. The aim of this research was to study the accuracy to which each filter estimates the joint angles in a serial manipulator. Preliminary experiments show that estimates from both filters describes the angular variations of the serial manipulator accurately. However, the double stage Kalman filter estimates the joint angles more precisely when the movement is around the IMU x- and y-axis. Nevertheless, when the movement is around the IMU z-axis, both filters showed comparable RMSE values. Therefore, we suggest using double stage Kalman filter data fusion algorithm to monitor angles around serial manipulators joints. The results of this research will serve as a support for further research dealing with joint monitoring ranging from clinical applications like upper limb joints assessment and gait analysis to industrial applications like robot precision enhancement.

Acknowledgements

This project is carried out under the MOBIDOC scheme, funded by The Ministry of Higher Education and Scientific Research through the PromEssE project and managed by the ANPR.

References

Choi D-Yun, Min H-K, Yong S-O, Soo-Ho J, Jae H-J, Hyung J-S, Hyung W-L, and Hye M-L (2017) Highly Stretchable, Hysteresis-Free Ionic Liquid-Based Strain Sensor for Precise Human Motion Monitoring, ACS Applied Materials & Interfaces 9, no. 2 (January 18, 2017).

Colton S (2007) The balance filter: a simple solution for integrating accelerometer and gyroscope measurements for a balancing platform. Chief Delphi white paper. 2007 Jun 25;1.

Denavit J, Hartenberg RS (1955) A kinematic notation for lower-pair mechanisms based on matrices, Trans ASME J. Appl. Mech. 23: 215–221.

Gui P, Tang L, and Mukhopadhyay S, (2015) MEMS based IMU for tilting measurement: Comparison of complementary and Kalman filter-based data fusion. 2015 IEEE 10th Conference on Industrial Electronics and Applications (ICIEA), 2004–2009. https://doi.org/10.1109/ICIEA.2015.7334442.

Interlink Inc (2011) SCORBOT-ER 9Pro User's Manual, Catalog # 200034 Rev. B March 2011.

Kalman RE (1960) A New Approach to Linear Filtering and Prediction Problems, Journal of Basic Engineering 82, 35–45.

Littrell ME, Chang Y-H, Selgrade BP (2018) Development and Assessment of a Low-Cost Clinical Gait Analysis System, Journal of Applied Biomechanics. 2018;34(6):503-508. doi:10.1123/jab.2017-0370

NovAtel (2014) IMU errors and their effects. [Online]. Available: https://hexagondownloads.blob.core.windows.net/public/Novatel/assets/Documents/Bulletins/APN064/APN064.pdf

Pedley M (2013) Tilt Sensing Using a Three-Axis Accelerometer, Freescale Semiconductor Application Note, AN3461, 03, 2013.

Sabatelli S, Galgani M, Fanucci L, Rocchi A (2012) A double stage Kalman filter for sensor fusion and orientation tracking in 9D IMU, In: 2012 IEEE Sensors Applications Symposium Proceedings. 2012 IEEE Sensors Applications Symposium (SAS), Brescia, Italy: IEEE, pp. 1–5.doi:10.1109/SAS.2012.6166315.

Wu J, Zhou Z, Fourati H, Li R, Liu M (2019) Generalized Linear Quaternion Complementary Filter for Attitude Estimation from Multi-Sensor Observations: An Optimization Approach. *IEEE Transactions on Automation Science and Engineering*. Published online 2019:1-14. doi:10.1109/TASE.2018.2888908.